J. Fluid Mech. (2005), *vol.* 522, *pp.* 101–116.
DOI: 10.1017/S0022112004001703 Printed in the United Kingdom

Viscous eddies in a circular cone

By V. S. MALYUGA†

Institute of Hydromechanics, National Academy of Sciences,
03680 Kiev, Ukraine

(Received 26 January 2004 and in revised form 4 August 2004)

The flow of viscous incompressible fluid in a circular cone induced by a non-zero velocity prescribed at the boundary within a ring $0 < a_1 < r < a_2 < \infty$, where r is the distance from the vertex, is considered in the limits of the Stokes approximation. In the spherical coordinate system (r, θ, ϕ) with the origin at the vertex and the axis $\theta = 0$ coincident with the axis of the cone the velocity and pressure fields are represented in the form of a Fourier series on the trigonometric system $\cos m\phi$. The solution is constructed for each term by use of the Mellin transform. The contribution of each term of the Fourier expansion to the local velocity field near the vertex is studied. The kinematics of the local flows is illustrated by two examples. The flows are induced by the motion of two and three equally spaced segments, respectively.

1. Introduction

Creeping flows of viscous incompressible fluid in the neighbourhood of singular points of a rigid boundary are of traditional interest. Such flows may be considered within the limits of the linear approximation (Stokes flow), since the inertial forces are negligible in comparison with the viscous forces (Moffatt 1964*a*).

The Stokes flow in the neighbourhood of a smooth edge (a line of intersection of two smooth surfaces) has been thoroughly studied. This problem can be traced back to Goodier (1934) and Taylor (1962) who considered the flow induced in a wedge by the steady motion of a wall in the tangential direction. The solution of the two-dimensional problem of the Stokes flow induced in a corner with rigid sides by a general motion at a large distance from the corner was presented by Dean & Montagnon (1949). Later Moffatt (1964*a*, *b*) interpreted their results as follows: if the corner is sufficiently acute, there exists an infinite sequence of eddies. Their dimensions and the intensities decrease in geometric progression as the corner is approached. Using the Mellin transform technique, he constructed the solution for a particular example of flow excitation (Moffatt 1964*b*). The flow was induced by the motion of segments (sleeves) situated at the walls. More recently, Moffatt & Duffy (1980) studied the pressure-driven flow directed along the edge (Poiseuille flow) and analysed the breakdown of the local similarity solution. The instantaneous Stokes flow in a corner between two free surfaces under the action of gravity parallel to the bisectrix was studied by Betelú *et al.* (1996). Neglecting the surface tension, they found the range of angles in which the dominant term of the solution is independent of gravity and represents a similarity solution of the second type, and thus a sequence

† Present address: Netherlands Institute of Ecology (NIOO-KNAW), Centre for Estuarine and Marine Ecology, Department of Ecosystem Studies, Korringaweg 7, 4401 NT Yerseke, The Netherlands.

of Moffatt eddies may exist. The breakdown of the local similarity solution in a wedge formed by a rigid wall and a surface of constant shear stress was studied by Kuhlmann, Nienhüser & Rath (1999).

The axisymmetric Stokes flow has also been studied extensively. First, the paper by Wakiya (1976) should be mentioned. He studied the eigenfunction flows in a conical domain and established that for the semi-angle of the cone less than about 80.9° the first root of the eigenvalue equation is complex and consequently an infinite sequence of eddies is induced near the apex. At about the same time Liu & Joseph (1978) considered the axisymmetric flow in conical trenches and showed that a sequence of toroidal eddies exists near the vertex provided the opening angle is less than a critical value. Secondary flows between two cones, the inner one rotating, were discussed by Moffatt (1980), paying particular attention to toroidal vortices, which occur for a certain range of angles of the cones. Recently, Weidman & Calmidi (1999) studied the axisymmetric instantaneous Stokes flow in a conical domain bounded by a free surface. The fluid was acted upon by gravity parallel to the conical axis. The range of angles was found for which the dominant term of the solution was independent of gravity and exhibited properties qualitatively similar to those of the steady axisymmetric flow in a rigid cone reported by Liu & Joseph (1978).

Thus there exists a large body of research into plane and axisymmetric Stokes flows near a corner and conical singular points of a boundary. The situation with three-dimensional flows is quite different. Although the mathematical aspects have been thoroughly studied (see Kozlov, Maz'ya & Rossmann 2001 for further mathematical details), there are only a few papers which deal with three-dimensional velocity fields in such domains. The flow in a corner region was studied by Moffatt & Mak (1999) under the assumption that the velocity field weakly varied along the edge. It was shown that in a flow antisymmetric about the bisecting plane, the part of the velocity oscillating with the distance from the edge dominates and thus the flow exhibits the eddy structure. In symmetric flow, however, the non-oscillating part was dominant. The same conclusion was drawn earlier by Sano & Hasimoto (1980) who considered the flow in a corner driven by a Stokeslet. In recent years the domain of a trihedral corner has been one of the more intriguing geometries. Hills & Moffatt (2000) considered a more general problem. The domain was bounded by two fixed rigid triangular 'fins' inserted into a circular cone and a rotating conical surface. In the special case that the angle of the cone is $\gamma = \pi/2$, this domain turns into a semi-infinite wedge. The authors focused their attention on the asymptotic flow near the edge formed by the immovable fins and concluded that, provided the angle between the fins is less than a critical angle, an infinite sequence of eddies would be generated near the edge. More recently, Gomilko, Malyuga & Meleshko (2003) constructed the solution of the boundary-value problem in a trihedral rectangular corner. The flow was generated by the motion of a wall. The authors employed the method of superposition, considering the corner as the intersection of three half-sectors of a solid sphere with the centre at the vertex of the corner. Combining analytical reasoning and numerical simulations, they confirmed the asymptotic analysis by Hills & Moffatt (2000). It was also shown that, if the movable wall rotates about a centre displaced from the vertex, the three-dimensionality of the flow becomes significant. A stagnation line composed of both saddles and centres was found. Shankar (2000) considered another problem. The flow in a semi-infinite wedge was generated by a non-zero velocity distributed over the boundary within some strip $0 < a_1 < r < a_2 < \infty$, where r is a distance from the vertex. Particular attention was given to the existence of eddies near the edge formed by two stationary planes. Thus the asymptotic flow

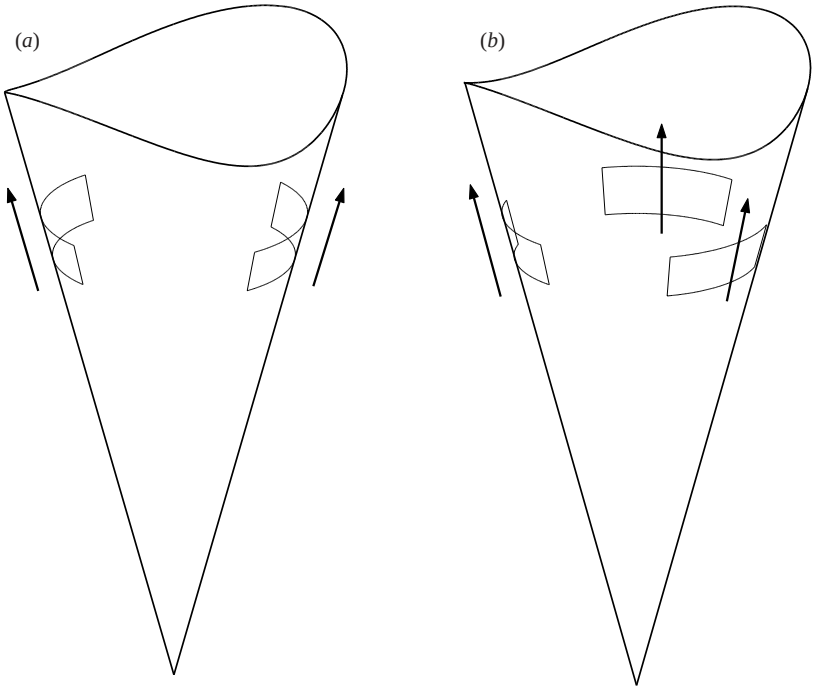

FIGURE 1. Geometry of the problem. Examples of the boundary condition: (*a*) the motion of two identical segments symmetric about the axis of the cone, (*b*) the motion of three identical equally spaced segments.

near the vertex of a trihedral corner induced by an arbitrary velocity applied at a large distance from the vertex still remains a challenge. It is natural to expect that such flow might represent a sequence of eddies even in the case that eddies do not exist near the edges owing to the dominant role of the Poiseuille flow in a dihedral corner (Moffatt & Duffy 1980).

In the present paper we consider a simplified problem. The steady Stokes flow in a circular cone is induced by a non-zero tangential velocity prescribed at the conical surface within a ring $0 < a_1 < r < a_2 < \infty$ (figure 1). The simplicity of the problem allows us to concentrate our attention on the behaviour of the flow near the vertex. In the spherical coordinate system (r, θ, ϕ) with the origin at the vertex and the axis $\theta = 0$ coincident with the axis of the cone, the boundary condition is represented in the form of a Fourier series on the trigonometric system $\cos m\phi$. The contribution of each term of the Fourier expansion to the asymptotic flow near the vertex is studied separately. By way of example we consider two flows induced by the motion of two and three equally spaced segments of the ring $a_1 < r < a_2$ (figure 1). In the first case the asymptotic flow near the vertex is determined by the dominant role of the term at $m = 2$, while in the latter case by the term at $m = 0$.

When reproducing this forcing experimentally, the moving surfaces (sleeves) must be made of elastic material, since the curvature changes with r. One might expect that streamline patterns near the vertex similar to those presented here can also be obtained using another type of fluid agitation. For example, the flow may be driven by two or three equally spaced spheres situate in the fluid near the conical surface.

The paper is organized as follows: the formulation of the problem and the general representation of its solution are given in § 2 for each term of the Fourier expansion

of the general boundary condition. The asymptotic flows near the vertex and far away from both the vertex and the ring of excitation are discussed in § 3. Two flows induced by more general distributions of the prescribed velocity, which include infinitely many terms of the Fourier expansion, are studied in § 4. Some conclusions mainly concerning the role of different terms of the Fourier expansion in the local velocity field near the vertex are given in § 5. Appendix A contains the asymptotic expansions of the associated Legendre functions for small angle and large degree, and Appendix B contains the coefficients of the velocity field in an infinite cylinder, which is the limiting case of the cone.

2. Statement of the problem and general representation of its solution

2.1. *Problem formulation*

Let us consider a three-dimensional creeping flow of an incompressible viscous fluid in a cone of a circular cross-section $0 \leqslant r < \infty$, $0 \leqslant \theta \leqslant \alpha$, $0 \leqslant \phi \leqslant 2\pi$, where (r, θ, ϕ) is the spherical coordinate system with the origin at the vertex of the cone. The flow is governed by the Stokes equations

$$\mu \nabla^2 \boldsymbol{U} = \nabla P, \qquad \nabla \cdot \boldsymbol{U} = 0, \tag{2.1a, b}$$

where $\boldsymbol{U}$ and P are velocity and pressure fields, respectively, and μ is the shear viscosity of the fluid.

The motion of the fluid is generated by a tangential velocity U_r distributed over a region $a_1 \leqslant r \leqslant a_2$ of the boundary $\theta = \alpha$. The boundary condition for the component U_r of the velocity vector is given as follows:

$$U_r = \begin{cases} f_m(r) \cos m\phi & \text{at} \quad a_1 \leqslant r \leqslant a_2, \quad \theta = \alpha, \quad 0 \leqslant \phi \leqslant 2\pi, \\ 0 & \text{at} \quad r < a_1 \quad \text{or} \quad r > a_2, \quad \theta = \alpha, \quad 0 \leqslant \phi \leqslant 2\pi, \end{cases} \tag{2.2}$$

with $m = 0, 1, 2, \ldots$. Here $f_m(r)$ is an arbitrary smooth function. The other components are prescribed to be zero over the whole boundary. In a more general case the boundary condition can be represented in the form of Fourier series on the complete trigonometric system $\cos m\phi$ and $\sin m\phi$ with $m = 0, 1, 2, \ldots$. Owing to the circular geometry of the problem, the boundary condition $f_m(r) \sin m\phi$ can be readily reduced to the boundary condition (2.2) through rotation of the coordinate system $\phi = \psi + \pi/2m$. In view of the linearity of the problem, a more general velocity can be represented as a sum of the solutions of problem (2.1), (2.2) at various m.

2.2. *General representation of the solution*

First we consider a particular solution of equation (2.1), which is of a simple form, and then progress to the general representation, which enables one to satisfy the boundary conditions (2.2) with arbitrary function $f_m(r)$.

Because of the structure of the boundary conditions, we may seek a solution of the form

$$\left.\begin{aligned} P &= \mu r^{\lambda-1} p_m(\theta, \lambda) \cos m\phi, & U_r &= r^\lambda q_m(\theta, \lambda) \cos m\phi, \\ U_\theta &= r^\lambda s_m(\theta, \lambda) \cos m\phi, & U_\phi &= r^\lambda t_m(\theta, \lambda) \sin m\phi, \end{aligned}\right\} \tag{2.3}$$

where λ is an arbitrary parameter. The substitution of (2.3) into the governing equations (2.1) provides the system of ordinary differential equations, from which the unknown functions p_m, q_m, s_m and t_m can be found. Since these equations are rather

cumbersome and require additional manipulations, a more convenient way is to use the representation of the velocity and pressure field in terms of three spherical harmonics

$$\left.\begin{aligned} P &= \mu p_{\lambda-1}, \\ \boldsymbol{U} &= \nabla\times(\boldsymbol{r}\chi_\lambda) + \nabla\Phi_{\lambda+1} + \frac{\lambda+2}{2\lambda(2\lambda+1)}\, r^2\nabla p_{\lambda-1} - \frac{\lambda-1}{\lambda(2\lambda+1)}\,\boldsymbol{r}\, p_{\lambda-1}, \end{aligned}\right\} \tag{2.4}$$

where $\Phi_{\lambda+1}$, χ_λ and $p_{\lambda-1}$ are three solid spherical harmonics of degrees $\lambda+1$, λ and $\lambda-1$, respectively. Representation (2.4) has a structure similar to the representation of the velocity and pressure fields derived by Gomilko *et al.* (2003, (3.5)) from the well-known Lamb's solution of the Stokes problem in spherical coordinates (Lamb 1932). The difference is that the solution by Gomilko *et al.* contained only the spherical harmonics of integer degrees, which was caused by the polynomial dependence of the boundary conditions on r. For the problem under consideration it is necessary to take the spherical harmonics of arbitrary complex degrees. It is evident that representation (2.4) remains valid for complex λ.

The spherical harmonics can be chosen in the following form:

$$\left.\begin{aligned} \Phi_{\lambda+1} &= X_m^{(1)}(\lambda)\, r^{\lambda+1}\, P_{\lambda+1}^{-m}(\cos\theta)\,\cos(m\phi), \\ \chi_\lambda &= X_m^{(2)}(\lambda)\, r^{\lambda}\, P_{\lambda}^{-m}(\cos\theta)\,\sin(m\phi), \\ p_{\lambda-1} &= X_m^{(3)}(\lambda)\, r^{\lambda-1}\, P_{\lambda-1}^{-m}(\cos\theta)\,\cos(m\phi), \end{aligned}\right\} \tag{2.5}$$

with three unknown coefficients $X_m^{(1)}$, $X_m^{(2)}$ and $X_m^{(3)}$, which depend on the parameter λ. Here $P_\nu^{-m}(\cos\theta)$ denotes the associated Legendre functions of the first kind.† Now, substituting (2.5) into (2.4) and comparing the result with representation (2.3), one can obtain the following relations for the unknown functions:

$$\left.\begin{aligned} p_m &= X_m^{(3)} P_{\lambda-1}^{-m}(\cos\theta), \\ q_m &= (\lambda+1)X_m^{(1)} P_{\lambda+1}^{-m}(\cos\theta) + \frac{\lambda-1}{2(2\lambda+1)} X_m^{(3)} P_{\lambda-1}^{-m}(\cos\theta), \\ s_m &= X_m^{(1)} P_{\lambda+1}^{-m\,\prime}(\cos\theta) + X_m^{(2)} \frac{m\, P_\lambda^{-m}(\cos\theta)}{\sin\theta} + \frac{\lambda+2}{2\lambda(2\lambda+1)} X_m^{(3)} P_{\lambda-1}^{-m\,\prime}(\cos\theta), \\ t_m &= -X_m^{(1)} \frac{m\, P_{\lambda+1}^{-m}(\cos\theta)}{\sin\theta} - X_m^{(2)} P_\lambda^{-m\,\prime}(\cos\theta) - \frac{\lambda+2}{2\lambda(2\lambda+1)} X_m^{(3)} \frac{m\, P_{\lambda-1}^{-m}(\cos\theta)}{\sin\theta}. \end{aligned}\right\} \tag{2.6}$$

Here and in what follows the prime denotes a derivative with respect to θ.

The integration of (2.3) with respect to the parameter λ along a contour parallel to the imaginary axis provides a representation of the solution in the form of the inverse Mellin transform, which allows one to satisfy the general boundary condition (2.2):

$$\left.\begin{aligned} P &= \frac{\mu\,\cos m\phi}{2\pi\mathrm{i}} \int_{\sigma-\mathrm{i}\infty}^{\sigma+\mathrm{i}\infty} r^{\lambda-1}\, p_m(\theta,\lambda)\,\mathrm{d}\lambda, \qquad U_r = \frac{\cos m\phi}{2\pi\mathrm{i}} \int_{\sigma-\mathrm{i}\infty}^{\sigma+\mathrm{i}\infty} r^{\lambda}\, q_m(\theta,\lambda)\,\mathrm{d}\lambda, \\ U_\theta &= \frac{\cos m\phi}{2\pi\mathrm{i}} \int_{\sigma-\mathrm{i}\infty}^{\sigma+\mathrm{i}\infty} r^{\lambda}\, s_m(\theta,\lambda)\,\mathrm{d}\lambda, \qquad U_\phi = \frac{\sin m\phi}{2\pi\mathrm{i}} \int_{\sigma-\mathrm{i}\infty}^{\sigma+\mathrm{i}\infty} r^{\lambda}\, t_m(\theta,\lambda)\,\mathrm{d}\lambda. \end{aligned}\right\} \tag{2.7}$$

† The associated Legendre functions of negative integer order $-m$ are used. This choice will allow us to avoid additional mathematical treatments at integer values of λ, at which the functions of positive order become identically zero: $P_n^m(\cos\theta)\equiv 0,\ m = n+1,\ n+2,\ldots$.

Here σ is chosen so that the integral $\int_0^\infty r^{-\sigma-1}\,\boldsymbol{U}\,\mathrm{d}r$ exists. Since the velocity prescribed at the boundary is non-zero only within a finite strip away from the vertex, the velocity in the cone vanishes both at the vertex and at infinity, say $|\boldsymbol{U}| = O(r^{\sigma_1}),\quad r \to 0,\quad \sigma_1 > 0$ and $|\boldsymbol{U}| = O(r^{\sigma_1^*}),\quad r \to \infty,\quad \sigma_1^* < 0$ (σ_1 and σ_1^* will be found later). It is evident that σ can be any real constant from the interval (σ_1^*, σ_1).

2.3. *Satisfaction of the boundary condition*

The unknown coefficients $X_m^{(1)}$, $X_m^{(2)}$ and $X_m^{(3)}$ are to be determined from the boundary conditions (2.2). The Mellin transform taken at the boundary $\theta = \alpha$ provides the following linear algebraic system:

$$\left.\begin{aligned} &q_m(\alpha, \lambda) = \int_{a_1}^{a_2} f_m(r)\, r^{-\lambda-1}\mathrm{d}r \equiv F_m(\lambda),\\ &s_m(\alpha, \lambda) = 0,\\ &t_m(\alpha, \lambda) = 0. \end{aligned}\right\} \tag{2.8}$$

The unknown coefficients are determined from this system as follows:

$$X_m^{(i)}(\lambda) = F_m(\lambda)\,\frac{\Delta_m^{(i)}(\lambda)}{\Delta_m(\lambda)}, \quad i = 1, 2, 3, \tag{2.9}$$

where the determinant Δ_m and the algebraic adjuncts $\Delta_m^{(i)}$ are

$$\Delta_m = (\lambda+1)\,P_{\lambda+1}^{-m}\,\Delta_m^{(1)}(\lambda) + \frac{\lambda-1}{2(2\lambda+1)}\,P_{\lambda-1}^{-m}\,\Delta_m^{(3)}(\lambda), \tag{2.10}$$

$$\left.\begin{aligned} \Delta_m^{(1)} &= \frac{\lambda+2}{2\lambda(2\lambda+1)}\left[P_{\lambda-1}^{-m\prime}\,P_\lambda^{-m\prime} - \frac{m^2}{\sin^2\alpha}\,P_{\lambda-1}^{-m}\,P_\lambda^{-m}\right],\\ \Delta_m^{(2)} &= \frac{\lambda+2}{2\lambda(2\lambda+1)}\,\frac{m}{\sin\alpha}\left[P_{\lambda+1}^{-m\prime}\,P_{\lambda-1}^{-m} - P_{\lambda+1}^{-m}\,P_{\lambda-1}^{-m\prime}\right],\\ \Delta_m^{(3)} &= -P_{\lambda+1}^{-m\prime}\,P_\lambda^{-m\prime} + \frac{m^2}{\sin^2\alpha}\,P_{\lambda+1}^{-m}\,P_\lambda^{-m}. \end{aligned}\right\} \tag{2.11}$$

Here and in what follows, for brevity, the constant argument $\cos\alpha$ of the associated Legendre functions is omitted.

3. Asymptotic behaviour of the flow at small and large r

3.1. *Flow near the vertex of a cone*

The behaviour of the flow near the vertex is characterized by the location of the roots of the equation

$$\Delta_m(\lambda) = 0 \tag{3.1}$$

in the right-hand half of the complex plane, at which the integrands in (2.7) have poles, which are generally simple. Completing the contour of integration in (2.7) in the half-plane $\mathrm{Re}\lambda > 0$ at a large distance from the origin and applying the theorem of residues, we obtain a representation for the velocity in the domain $r < a_1$ in the form of the sum of residues. Since λ_1 (the solution of equation (3.1) with a smallest positive real part) determines the asymptotic behaviour of the flow near the vertex,

2α (deg.)	m	ξ_1	η_1	$\ln\rho_1$	$\ln\omega_1$	2α (deg.)	m	ξ_1	η_1	$\ln\rho_1$	$\ln\omega_1$
0	0	8.93	2.94	0.00	9.56	90	0	8.23	2.46	2.00	10.49
	1	5.14	2.25	0.00	7.19		1	4.63	1.79	2.75	8.11
	2	7.83	2.62	0.00	9.37		2	7.41	2.18	2.27	10.70
10	0	8.85	2.93	0.19	9.49	110	0	8.10	2.19	2.76	11.63
	1	5.05	2.24	0.25	7.09		1	4.59	1.52	3.97	9.50
	2	7.75	2.62	0.21	9.29		2	7.42	1.91	3.16	12.23
30	0	8.68	2.89	0.57	9.45	130	0	7.99	1.79	3.98	14.00
	1	4.90	2.20	0.75	7.01		1	4.58	1.10	6.47	13.06
	2	7.61	2.58	0.64	9.27		2	7.48	1.51	4.71	15.52
50	0	8.52	2.80	0.98	9.56	150	0	7.90	1.14	7.19	21.70
	1	4.78	2.12	1.30	7.10		1	4.33	0.00	–	–
	2	7.50	2.50	1.10	9.45		2	7.58	0.81	10.12	29.29

TABLE 1. Values of $\xi_1 = 2\alpha\sigma_1$ and $\eta_1 = 2\alpha\tau_1$, where $\lambda_1 = \sigma_1 + i\tau_1$ is the principal root of equation (3.1). Length and intensity scale factors for the eddies.

the local velocity and pressure take the form

$$\left.\begin{aligned} P^{loc} &= \mu\, r^{\lambda_1 - 1}\, p_m(\theta, \lambda_1)\cos m\phi, & U_r^{loc} &= r^{\lambda_1}\, q_m(\theta, \lambda_1)\cos m\phi, \\ U_\theta^{loc} &= r^{\lambda_1}\, s_m(\theta, \lambda_1)\cos m\phi, & U_\phi^{loc} &= r^{\lambda_1}\, t_m(\theta, \lambda_1)\sin m\phi, \end{aligned}\right\} \tag{3.2}$$

where the functions p_m, q_m, s_m and t_m are given by (2.6) but the coefficients are now defined as follows:

$$X_m^{(i)}(\lambda) = -2F_m(\lambda)\,\frac{\Delta_m^{(i)}(\lambda)}{\Delta_m'(\lambda)}, \quad i = 1, 2, 3. \tag{3.3}$$

Here the prime denotes the derivative. If λ_1 is complex, the real part of (3.1) is understood to be relevant.

In the axisymmetric case ($m = 0$) the characteristic equation (3.1) is considerably simplified and takes the form

$$(\lambda - 1)\,\lambda\, P_{\lambda-1}\, P'_{\lambda+1} = (\lambda + 1)(\lambda + 2)\, P'_{\lambda-1}\, P_{\lambda+1}. \tag{3.4}$$

The root $\lambda = 1$ is evident. Since it is also a zero of the numerator in (2.6), it gives only a removable singularity of the integrands.

The characteristic equation (3.1) has both complex and real roots. The first eigenvalue $\lambda_1 = \sigma_1 + i\tau_1$, i.e. the eigenvalue with smallest positive real part, is of particular interest. The values of $\xi_1 = 2\alpha\sigma_1$ and $\eta_1 = 2\alpha\tau_1$ at various α are presented in table 1. At $m = 0$ and $m = 1$ they may be compared with the corresponding values of ξ_1 and η_1 in a two-dimensional corner in the symmetric and antisymmetric cases, respectively, given in Moffatt (1964*a*, table 1) for $2\alpha < 180°$. Indeed, at $m = 0$ the flow in any plane passing through the axis of the cone is two-dimensional and symmetric, and therefore it is expected to bear a resemblance to the symmetric flow in a two-dimensional corner of the same angle. At $m = 1$ the plane $\sin\phi = 0$ is the plane of symmetry. The flow in it is two-dimensional and antisymmetric. Thus it should be akin to the antisymmetric flow in the plane corner. As can be seen from table 1, in both the cases ξ_1 is slightly higher in a cone. As α increases, ξ_1 decreases in a cone and increases in a corner. Thus the difference is most distinct at low values of α. Obviously at $m \geqslant 2$ a comparison with two-dimensional flows is meaningless, since the three-dimensionality of the boundary conditions becomes significant.

m	0	1	2	3	4	5
$2\alpha_c$ (deg.)	161.7	148.9	157.2	161.1	163.5	165.2
ξ_1	7.86	4.60	7.63	10.64	13.66	16.69

TABLE 2. Critical angles $2\alpha_c$ and the corresponding values of ξ_1.

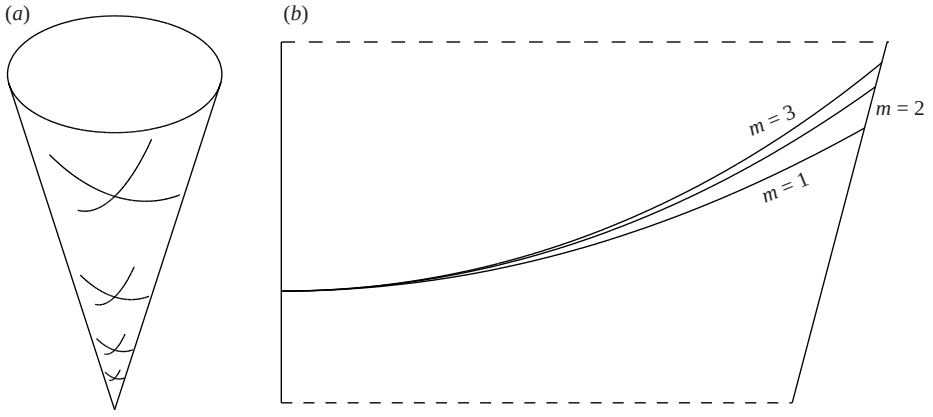

FIGURE 2. Centrelines of eddies. (*a*) The general view at $m=2$. (*b*) The centrelines at $m=1, 2, 3$ situated in the planes $\phi=\pi/2m$.

Similarly to the case of a plane corner, λ_1 is complex if α is less than some critical value and real if α exceeds it. This circumstance leads to the identical conclusion. Providing α is less than a critical value, there exists a sequence of eddies near the vertex. At $m=0$ and $m=1$ the critical angles (table 2) are greater only by 6° and 3°, respectively, than the critical angles of the symmetric and antisymmetric flows in a corner.

If $m>0$, the centrelines of the eddies lie in the planes $\phi=\pi(2k-1)/2m\equiv\phi_k$, $k=1, 2, \ldots, m$, in which the two components of the local velocity $U_r^{loc}=U_\theta^{loc}\equiv 0$. Following the analysis by Moffatt (1964), it is not difficult to show that the third component U_ϕ^{loc} has zeros at

$$r = r_0 \mathrm{e}^{-(\epsilon+n\pi)/\tau_1} \equiv r_n, \tag{3.5}$$

where r_0 is a length scale ($r_0 \ll a_1$) and ϵ is introduced so that

$$\sin\epsilon = \frac{\mathrm{Re}\left(A_m r_0^{\lambda_1} \tilde{t_m}\right)}{\left|A_m r_0^{\lambda_1} \tilde{t_m}\right|}, \qquad \cos\epsilon = -\frac{\mathrm{Im}\left(A_m r_0^{\lambda_1} \tilde{t_m}\right)}{\left|A_m r_0^{\lambda_1} \tilde{t_m}\right|}. \tag{3.6}$$

Equation (3.5) leads to the following conclusion. In the direction towards the vertex the dimensions of successive eddies decrease in geometric progression with ratio $\rho_1=\mathrm{e}^{\pi/\tau_1}$, which depends only on the angle 2α and m.

Since ϵ is a function of θ, relation (3.5) is the equation of the centrelines of eddies in the planes $\phi=\phi_k$. These lines calculated numerically at $m=2$ are represented in figure 2(*a*). The three-dimensionality of the domain is manifested in the curvilinear shape of the centrelines. In figure 2(*b*) the centrelines at $m=1, 2, 3$ are shown in planes $\phi=\pi/2m$. The scale factors r_0 are chosen so that the lines intersect at the axis of the cone. The greater is m, the higher is the end of the line, which means that the curvature grows with m.

2α (deg.)	m	ξ_1	2α (deg.)	m	ξ_1	2α (deg.)	m	ξ_1
10	3	10.24	90	3	10.03	150	3	10.48
	4	12.63		4	12.58		4	13.36
	5	14.97		5	15.08		5	16.21

TABLE 3. Values of ξ_1 at higher m.

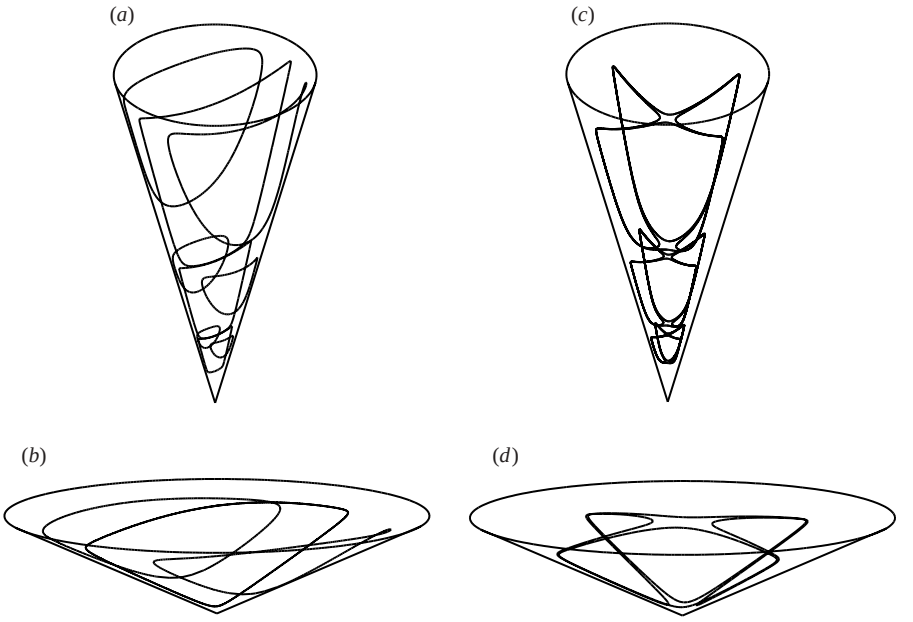

FIGURE 3. Streamline patterns. (*a*) $m=1$, $2\alpha=30^\circ$; (*b*) $m=1$, $2\alpha=130^\circ$; (*c*) $m=2$, $2\alpha=30^\circ$; (*d*) $m=2$, $2\alpha=130^\circ$.

The intensities of eddies also decrease in geometric progression. The ratio of intensities of successive (towards the vertex) eddies is $\omega_1=e^{\pi\sigma_1/\tau_1}$. The logarithms of ρ_1 and ω_1 are given in table 1. Comparison of their values with those in the corresponding two-dimensional flows (Moffatt 1964*a*), shows that ρ_1 is lower in a cone. Thus the dimensions of the eddies decrease as the vertex is approached more slowly. The intensity scale factor ω_1 is higher in a cone provided the angle α is sufficiently acute and lower as α increases.

For $m>0$, ξ_1 grows with increasing m. Comparing its values at higher m given in table 3 with the data in table 1, we may conclude that, when considered as a function of m, $\xi_1=\xi_1(m)$ obeys the inequality

$$\xi_1(1)<\xi_1(2)<\xi_1(0)<\xi_1(3)<\xi_1(4)<\ \ldots. \tag{3.7}$$

Hence, in the case of a general boundary condition represented in the form of Fourier series of the trigonometric functions $\cos m\phi$, the term at $m=1$ will dominate near the vertex or if this term is missing in the Fourier expansion, the term at $m=2$ will dominate.

The streamline patterns at $m=1$ and $m=2$ in cones of angles $2\alpha=30^\circ$ and $2\alpha=130^\circ$ are shown in figure 3. When the angle is acute, several successive eddies are observed, since the length scale factor ρ_1 is still sufficiently small. In the case $2\alpha=130^\circ$

the streamlines of only one eddy are represented, since the dimensions of eddies decay very rapidly as the vertex is approached ($\rho_1 = e^{6.468}$ at $m = 1$). Owing to the symmetries of the local velocity, all the streamlines are closed. For example, at $m = 2$ the streamlines situated in the first quarter ($0 \leqslant \phi \leqslant \pi/2$) are symmetric about the plane $\phi = \pi/4$, in which the centrelines of eddies lie.

3.2. *Special cases*

In the particular case of $2\alpha = \pi$-the cone turns into a half-space. The characteristic equation (3.1) is considerably simplified in this case. The eigenvalue λ_k can be found explicitly. Indeed, the associated Legendre functions and their derivatives take the following values (Abramowitz & Stegun 1965):

$$\left.\begin{aligned} P_\nu^\mu(0) &= \frac{2^\mu}{\sqrt{\pi}} \frac{\Gamma\left(\frac{1}{2}(\nu+\mu+1)\right)}{\Gamma\left(\frac{1}{2}(\nu-\mu)+1\right)} \cos\frac{\pi}{2}(\nu+\mu), \\ P_\nu^{\mu\,\prime}(0) &= -\frac{2^{\mu+1}}{\sqrt{\pi}} \frac{\Gamma\left(\frac{1}{2}(\nu+\mu)+1\right)}{\Gamma\left(\frac{1}{2}(\nu-\mu+1)\right)} \sin\frac{\pi}{2}(\nu+\mu), \end{aligned}\right\} \tag{3.8}$$

where Γ denotes the gamma function. Substituting (3.8) into (2.10), (2.11) and taking into account that the roots of Δ_m which are also the roots of $\Delta_m^{(i)}$ do not contribute to the local solution, we obtain the characteristic equation in the form

$$\frac{\lambda - m}{\lambda} \Gamma\left(\tfrac{1}{2}(\lambda - m)\right) \sin\left(\tfrac{1}{2}\pi(\lambda - m)\right) = 0 \tag{3.9}$$

with the roots

$$\lambda = m + 2k, \tag{3.10}$$

where $k = 0, 1, \ldots$ at $m > 0$ and $k = 1, 2, \ldots$ at $m = 0$.

Again, the local solution at $m = 1$ dominates. At $m = 0$ and $m = 2$ the first eigenvalues are equal and thus in a general case the leading role of one of these terms in the local velocity can be determined only by its leading role in the Fourier expansion of the boundary condition. The streamlines of the flow at $m = 2$ are represented in figure 4(*a*). Evidently, they are non-closed. No eddies appear in this case, since the critical angle $2\alpha_c < 180^\circ$.

Another special case is $\alpha \to 0$. The cone degenerates into an infinite cylinder. Taking the asymptotic values of the associated Legendre functions and their derivatives (Appendix A), the recurrence relations for the Bessel functions (Abramowitz & Stegun 1965) and the substitution $\gamma = \lambda\alpha$, we have from (2.10), (3.1) the characteristic equation

$$2\,J_{m-1}\,J_{m+1}(J_m + \gamma\,J_m') - \gamma\,J_m(J_{m-1}'\,J_{m+1} + J_{m-1}\,J_{m+1}') = 0. \tag{3.11}$$

Here the constant argument γ of the Bessel functions is omitted for brevity. The primes indicate differentiation with respect to the whole argument. Equation (3.11) first appeared in the fluid mechanics literature in Shankar (1997). The relevant solution (with a smallest positive real part) is complex. The values of $\xi_1 = 2\,\mathrm{Re}\gamma_1$ and $\eta_1 = 2\,\mathrm{Im}\gamma_1$ are given in table 1. They agree well with the eigenvalues presented in Shankar (1998). The eddies in the cylinder are all of the same dimension but their intensities decrease away from the region where a non-zero velocity is applied to the boundary. The three-dimensionality of the flow manifests itself in the greater values of the damping factor ω_1 than was observed in a layer between two rigid planes (Moffatt 1964*a*).

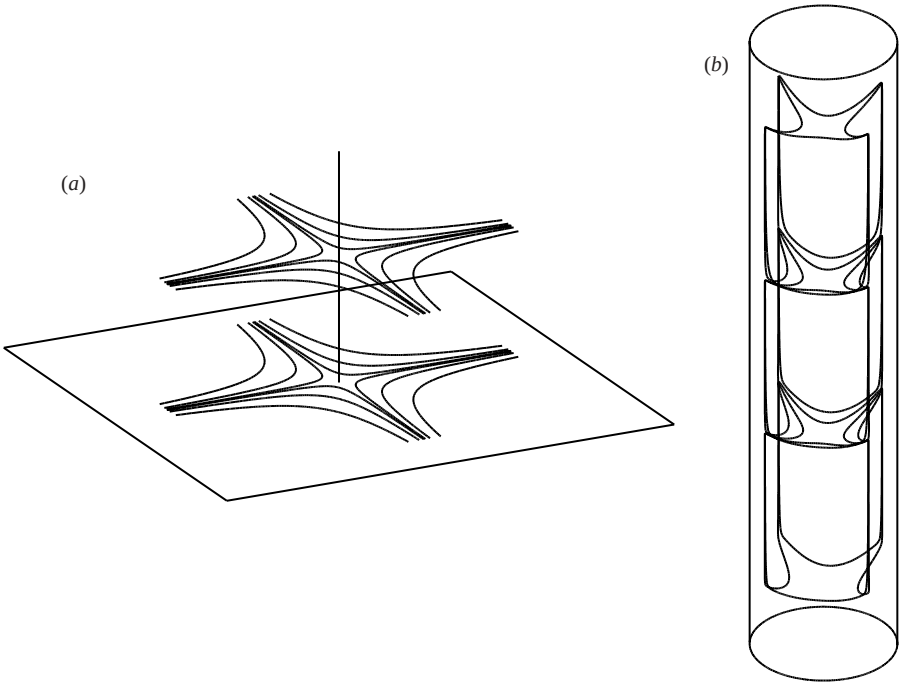

FIGURE 4. Streamline patterns at $m=2$. (*a*) $2\alpha=\pi$, the cone turns into a half-space; (*b*) $\alpha\to 0$, the cone turns into a cylinder.

The velocity field may be conveniently given in a cylindrical coordinate system (ρ,ϕ,z). For this purpose the origin of the system is chosen in the axis of the cone, which coincides with the Oz-axis, at a distance r_0 from the vertex. Fixing the cross-section of unit radius in the plane $z=0$ and letting α tend to zero, we obtain the following relations between the spherical and cylindrical coordinates:

$$r\sim z+r_0, \qquad \theta\sim\alpha\rho, \tag{3.12}$$

where $r_0\sim 1/\alpha$. Then the following asymptotic relation is valid:

$$\left(\frac{r}{r_0}\right)^{\lambda}\sim\left(1+\frac{z}{r_0}\right)^{\gamma/\alpha}\sim \mathrm{e}^{\gamma z}. \tag{3.13}$$

For the velocity components we have

$$U_\rho\sim U_\theta, \qquad U_z\sim U_r. \tag{3.14}$$

Then, from (3.2), (2.6), in view of (A 1), (A 2) and (3.12), we have the following expressions for the velocities in the infinite cylinder valid in the negative part ($z<0$), when the excitation is applied in the positive part ($z>0$):

$$\left.\begin{aligned} U_\rho &= u_\rho(\rho,\gamma_1)\,\mathrm{e}^{\gamma_1 z}\cos m\phi, \qquad U_\phi = u_\phi(\rho,\gamma_1)\,\mathrm{e}^{\gamma_1 z}\sin m\phi,\\ U_z &= \left[Y_m^{(1)}(\gamma_1)\,J_m(\gamma_1\rho)-Y_m(\gamma_1)\,\rho\,J_m'(\gamma_1\rho)\right]\,\mathrm{e}^{\gamma_1 z}\cos m\phi, \end{aligned}\right\} \tag{3.15}$$

where

$$\left.\begin{aligned} u_\rho+u_\phi &= Y_m^{(2)}(\gamma_1)\,J_{m+1}(\gamma_1\rho)+Y_m(\gamma_1)\,\rho\,J_{m+1}'(\gamma_1\rho),\\ u_\rho-u_\phi &= Y_m^{(3)}(\gamma_1)\,J_{m-1}(\gamma_1\rho)-Y_m(\gamma_1)\,\rho\,J_{m-1}'(\gamma_1\rho). \end{aligned}\right\} \tag{3.16}$$

The coefficients Y_m, $Y_m^{(i)}$ are given in Appendix B. The streamlines of this flow at $m=2$ are illustrated in figure 4(*b*). As already observed, the eddies are all of the same size but their intensities decrease with distance from the region of a non-zero boundary velocity.

3.3. *Flow at a large distance from the vertex*

To study the flow at a large distance from the vertex and from the region of excitation of the flow ($r \gg a_2$), the contour of integration in (2.7) should be completed in the left-hand half-plane $\mathrm{Re}\lambda < 0$ at a large distance from the origin. This asymptotic flow is governed by location of roots of (3.1) with negative real part. It should be noted that at $\lambda = 0$ and $\lambda = -1/2$ the integrands in (2.7) have only removable singularities.

The following property of the associated Legendre functions:

$$P_\lambda^{-m}(\cos\alpha) = P_{-\lambda-1}^{-m}(\cos\alpha) \tag{3.17}$$

allows one to relate the roots of (3.1) with positive and negative real parts. It follows from (2.10), (2.11), in view of (3.17), that

$$\Delta_m(-\lambda-1) = -\frac{\lambda}{\lambda+1}\,\Delta_m(\lambda). \tag{3.18}$$

Equation (3.18) suggests that the roots of (3.1) are symmetric about the straight line $\mathrm{Re}\lambda = -1/2$, i.e. if $\lambda = \lambda_k$ is a root of (3.1), then $\lambda = -\lambda_k - 1 \equiv \lambda_k^*$ is also a root of this equation. This fact, which is valid for Stokes flows in arbitrary conical domains (Kozlov *et al.* 2001, Theorem 5.2.1), comprises the principal difference between two-dimensional and three-dimensional flows. In a plane corner (Moffatt 1964*a*) the roots of the characteristic equation are symmetric about the imaginary axis $\mathrm{Re}\lambda = 0$. If angle α exceeds the limits 90° and $\simeq 126°$ for the antisymmetric and symmetric flows, respectively, then $\sigma_1 < 1$, and the Stokes approximation becomes invalid at a large distance from the corner, since the Reynolds number $Re = O(r^{\sigma_1^*+1}) = O(r^{-\sigma_1+1})$ increases with distance r. In a cone $\mathrm{Re} = O(r^{\sigma_1^*+1}) = O(r^{-\sigma_1})$. Thus at $r \gg a_2$ the contribution of the inertial forces may be neglected at any $m \geqslant 0$ and $0 < 2\alpha < 360°$.

4. Two examples of more general boundary conditions

When the boundary condition includes more than one term of the Fourier expansion in ϕ, the flow becomes more complicated. The general properties of such flows can be demonstrated with two typical examples, namely the flows induced by the motion of two and three equally spaced pieces of the strip $a_1 \leqslant r \leqslant a_2$ (flows A and B, respectively, see figure 1). To be specific, $a_1 = 1$, $a_2 = 1.1$ are taken. These problems have the following non-zero boundary conditions within this strip. Flow A:

$$U_r = 1, \qquad \tfrac{1}{4}\pi < \phi < \tfrac{3}{4}\pi \;\cup\; \tfrac{5}{4}\pi < \phi < \tfrac{7}{4}\pi. \tag{4.1}$$

Flow B:

$$U_r = 1, \qquad \tfrac{1}{6}\pi < \phi < \tfrac{3}{6}\pi \;\cup\; \tfrac{5}{6}\pi < \phi < \tfrac{7}{6}\pi \;\cup\; \tfrac{9}{6}\pi < \phi < \tfrac{11}{6}\pi. \tag{4.2}$$

The rest of the conical surface is fixed.

The non-zero Fourier coefficients of the boundary velocities are

$$f_0 = \tfrac{1}{2}, \qquad f_{2(2k-1)} = (-1)^k \frac{2}{(2k-1)\pi}, \qquad k = 1, 2, \ldots \tag{4.3}$$

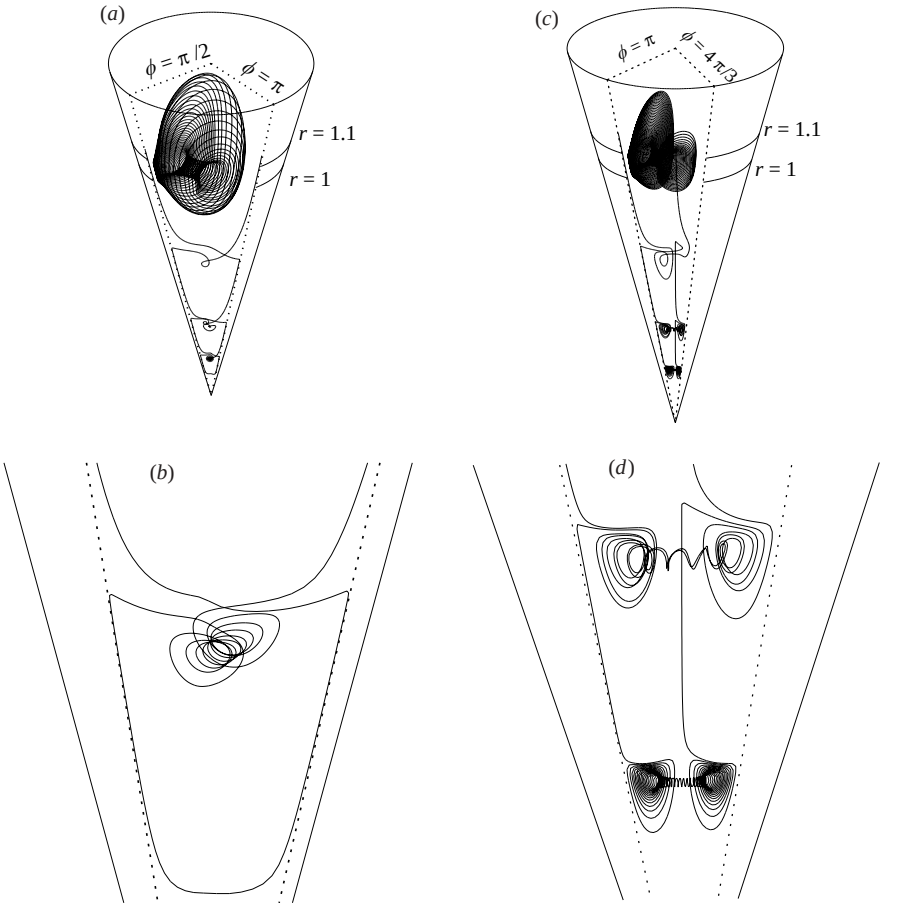

FIGURE 5. Streamline patterns, $2\alpha = 30°$. (*a*) Flow A. The general view. (*b*) Flow A. An enlarged view of the fourth eddy. (*c*) Flow B. The general view. (*d*) Flow B. An enlarged view of the third and fourth eddies.

for flow A and

$$f_0 = \tfrac{1}{2}, \qquad f_{3(2k-1)} = (-1)^k \frac{2}{(2k-1)\pi}, \qquad k = 1, 2, \ldots \tag{4.4}$$

for flow B. In both cases the dominant term ($m = 1$) is absent and hence the contribution of the terms $m = 0, 2, 3$ can be compared.

The general view of streamline patterns of flows A and B is represented in figures 5(*a*) and 5(*c*), respectively. In what follows the eddies are numbered starting with the primary (first) eddy, which is situated near the strip of non-zero boundary velocity. In the region of the eddies with higher numbers (second, third etc.) the Mellin integrals in (2.7) may be evaluated by the theorem of residues. For a cone of acute angle (in what follows $2\alpha = 30°$ is specified), the corresponding power series in r converge very rapidly. For example, at $m = 3$, $\sigma_1 = 19.31$ and $\sigma_2 = 29.99$, whereas at $m = 9$ (the third term in the Fourier expansion of flow B) $\sigma_1 = 45.76$. In the third eddy it is sufficient to take into account only the first eigenvalue λ_1 of the first two terms in the Fourier expansion.

In the region of the primary eddy, employment of the theorem of residues is inefficient to evaluate the Mellin integral in (2.7). A more appropriate procedure consists in the reduction of the contour integrals (2.7) to the real Fourier integrals. This technique is well-known. Since the contour of integration is parallel to the imaginary axis, $\mathrm{d}\lambda = \mathrm{i}\,\mathrm{d}\tau$. The Mellin transform of the Fourier coefficients f_m is

$$F_m(\lambda) = \frac{f_m}{\lambda}\left(a_1^{-\lambda} - a_2^{-\lambda}\right). \tag{4.5}$$

Separating the real and imaginary parts in (2.7) and taking into account that the real part is an even function of τ, we can rewrite the velocity as follows:

$$U_r = \sum_{m=0}^{\infty} \frac{f_m}{\pi} \cos m\phi \left[\left(\frac{r}{a_1}\right)^{\sigma} \int_0^{\infty} \left(R(\theta,\tau)\cos\tau\kappa_1 - T(\theta,\tau)\sin\tau\kappa_1\right) \mathrm{d}\tau \right.$$
$$\left. - \left(\frac{r}{a_2}\right)^{\sigma} \int_0^{\infty} \left(R(\theta,\tau)\cos\tau\kappa_2 - T(\theta,\tau)\sin\tau\kappa_2\right) \mathrm{d}\tau \right], \tag{4.6}$$

where

$$R(\theta,\tau) = \mathrm{Re}\left(\frac{q_m(\theta,\lambda)}{\lambda F_m(\lambda)}\right), \qquad T(\theta,\tau) = \mathrm{Im}\left(\frac{q_m(\theta,\lambda)}{\lambda F_m(\lambda)}\right), \qquad \kappa_i = \ln\frac{r}{a_i}. \tag{4.7}$$

The other components can be obtained by the same procedure.

The highest numerical error occurs in the vicinity of the lines, where the prescribed boundary velocity is discontinuous. Since the local solutions near these lines are known, it is possible in principle to get rid of the singularity (see, for example, Meleshko 1996), which allows one to considerably improve the satisfaction of the boundary conditions in this region. Since this procedure is useful only in the vicinity of the points of discontinuity and has an insignificant effect on the flows near the vertex and in the interior of the cone, it is outside the scope of this paper. In the Fourier series (4.6) 100 non-zero terms were retained. Two components U_θ and U_ϕ give identical zero at the boundary. For the component U_r, even in the small neighbourhood ($r = 0.999$) of the line $r = a_1 = 1$, the numerical error does not exceed 3% of the velocity prescribed at the boundary.

As a consequence of the velocity field symmetries, the streamlines of flows A and B are symmetric about the planes $\phi = \pi k/2$ and $\phi = \pi k/3$, respectively. Figures 5(a) and 5(c) illustrate only the streamline patterns situated in the quarter $\pi/2 < \phi < \pi$ and in the one sixth of the cone $\pi < \phi < 4\pi/3$. The streamline involved in the primary eddy has a complicated spiral shape. As it approaches the plane $\phi = \pi/2$ (figure 5a), the coils widen. Then it approaches the stationary part of the conical surface $3\pi/4 < \phi < \pi$, and the coils converge. The streamline involved in the primary eddy of flow B has a similar geometry. It should be mentioned that streamlines of spiral shape near a smooth edge have been reported earlier, e.g. Shankar (1997, 2000), Meleshko, Malyuga & Gomilko (2000).

In the eddies of higher numbers of flow A, where the second term ($m = 2$) of the Fourier expansion plays the dominant role, the streamlines wind round a line situated nearly in the plane $\phi = 3\pi/4$ (figure 5b). In flow B the dominance of the axisymmetric term ($m = 0$) is manifested in the appearance of comparatively large regions in which the streamlines wind nearly round the circle $r = \mathrm{const}$, $\theta = \mathrm{const}$ (figure 5d). The higher is the number of an eddy, the more tightly wound are the spirals.

5. Conclusions

The velocity and pressure fields of the Stokes flow in a circular cone driven by a non-zero velocity applied to the boundary within the ring $0 < a_1 < r < a_2 < \infty$ are represented in the form of Fourier series on the trigonometric system $\cos m\phi$. The problem is considered separately for each term of the Fourier expansion and the solution is constructed in the form of the Mellin integral.

The transcendental equation for the eigenvalues, which determine the asymptotic flow in the neighbourhood of the vertex, is obtained. The numerical analysis shows that at any m there exists a critical value of the opening angle, below which the first pair of eigenvalues are complex and above which they become real. This circumstance leads us to a conclusion similar to that drawn by Moffatt (1964*a*, *b*) for the two-dimensional flow in a plane corner. At any m, providing α is less than the critical value, there exists a sequence of eddies near the vertex.

Being considered as a function of m, the real part of the first eigenvalue $\xi_1 = \xi_1(m)$ obeys the inequality $\xi_1(1) < \xi_1(2) < \xi_1(0) < \xi_1(3) < \xi_1(4) < \dots$. Hence, when the Fourier expansion of the velocity prescribed at the boundary includes several terms, the term at $m = 1$ will dominate near the vertex. If this term is missing in the Fourier expansion, the term at $m = 2$ will dominate. If both the terms are missing, the axisymmetric term ($m = 0$) will play a leading role.

I am grateful to Professor V. V. Meleshko from Kiev University and Professor A. M. Gomilko from the Institute of Hydromechanics, Kiev for helpful discussions in the course of seminar 'Problems of mechanics' held by Professor V. T. Grinchenko and Professor A. F. Ulitko at Kiev University. I am indebted to Professor C. H. R. Heip and Professor J. B. M. Middelburg from the Centre for Estuarine and Marine Ecology, Yerseke for their hospitality and aid. My thanks also go to Professor H. K. Moffatt and an anonymous referee, whose suggestions led to improvements in presentation of the paper.

Appendix A

As $\alpha \to 0$, $\mathrm{Re}\lambda \to \infty$ and $\mathrm{Re}\lambda\alpha = O(1)$, the following asymptotic representations of the associated Legendre functions and their derivatives is valid (Gradshteyn & Ryzhik 2000):

$$\lambda^m P^{-m}_{\lambda+k}(\cos\alpha) = J_m(\lambda\alpha) - \frac{(2k+1)}{2} J_{m+1}(\lambda\alpha)\,\alpha + O(\alpha^2), \tag{A 1}$$

$$\lambda^{m-1} P^{-m\,\prime}_{\lambda+k}(\cos\alpha) = J'_m(\lambda\alpha) - \frac{(2k+1)}{2}\left(J'_{m+1}(\lambda\alpha) + \frac{1}{\lambda\alpha} J_{m+1}(\lambda\alpha)\right)\alpha + O(\alpha^2), \tag{A 2}$$

where $k = -1, 0, 1$; and J_μ, J'_μ denote the Bessel function of the first kind and its derivative with respect to the whole argument, respectively.

Appendix B

The coefficients of the velocity field in an infinite cylinder are

$$Y_m(\gamma) = -\gamma\left(Y_m^{(1)} + \tfrac{1}{2}\left(Y_m^{(2)} - Y_m^{(3)}\right)\right), \quad Y_m^{(i)}(\gamma) = G_m(\gamma)\frac{d_m^{(i)}(\gamma)}{d'_m(\gamma)}, \quad i = 1, 2, 3. \tag{B 1}$$

The determinant d_m and the algebraic adjuncts $d_m^{(i)}$ are given as follows:

$$\left.\begin{aligned} d_m^{(1)} &= J_{m-1}(\gamma)\,J_{m+1}(\gamma) - \tfrac{1}{2}\bigl(d_m^{(2)}(\gamma) - d_m^{(3)}(\gamma)\bigr), \quad d_m^{(2)} = \gamma\,J_{m-1}(\gamma)\,J'_{m+1}(\gamma), \\ d_m^{(3)} &= -\gamma\,J'_{m-1}(\gamma)\,J_{m+1}(\gamma), \quad d_m = \gamma\,J_{m-1}(\gamma)\,J'_m(\gamma)\,J_{m+1}(\gamma) + J_m(\gamma)\,d_m^{(1)}(\gamma); \end{aligned}\right\} \tag{B 2}$$

$$G_m(\gamma) = -2\int_{b_1}^{b_2} g_m(z)\,\mathrm{e}^{-\gamma z}\,\mathrm{d}z \tag{B 3}$$

where $g_m(z)$ is a non-zero velocity U_z prescribed at the boundary $\rho = 1$ within the strip $b_1 \leqslant z \leqslant b_2$.

REFERENCES

Abramowitz, M. & Stegun, I. A. 1965 *Handbook of Mathematical Functions*. Dover.

Betelú, S., Diez, J., Gratton, R. & Thomas, L. 1996 Instantaneous viscous flow in a corner bounded by free surfaces. *Phys. Fluids* **8**, 2269–2274.

Dean, W. R. & Montagnon, P. E. 1949 On the steady motion of viscous liquid in a corner. *Proc. Camb. Phil. Soc.* **45**, 389–395.

Gomilko, A. M., Malyuga, V. S. & Meleshko, V. V. 2003 On steady Stokes flow in a trihedral rectangular corner. *J. Fluid Mech.* **476**, 159–177.

Goodier, J. N. 1934 An analogy between the slow motion of a viscous fluid in two dimensions, and systems of plane stress. *Phil. Mag.* (7) **17**, 554–576.

Gradshteyn, I. S. & Ryzhik, I. M. 2000 *Table of Integrals, Series, and Products*, 6th edn. (ed. A. Jeffrey & D. Zwillinger). Academic.

Hills, C. P. & Moffatt, H. K. 2000 Rotary honing: a variant of the Taylor paint-scraper problem. *J. Fluid Mech.* **418**, 119–135.

Kozlov, V. A., Maz'ya V. G. & Rossmann, J. 2001 *Spectral Problems Associated with Corner Singularities of Solutions to Elliptic Equations*. American Mathematical Society.

Kuhlmann, H. C., Nienhüser, C. & Rath, H. J. 1999 The local flow in a wedge between a rigid wall and a surface of constant shear stress. *J. Engng Maths* **36**, 207–218.

Lamb, H. 1932 *Hydrodynamics*, 6th edn. Cambridge University Press.

Liu, C. H. & Joseph D. D. 1978 Stokes flow in conical trenches. *SIAM J. Appl. Maths* **34**, 286–296.

Meleshko, V. V. 1996 Steady Stokes flow in a rectangular cavity. *Proc. R. Soc. Lond.* A **452**, 1999–2022.

Meleshko, V. V., Malyuga, V. S. & Gomilko, A. M. 2000 Steady Stokes flow in a finite cylinder. *Proc. R. Soc. Lond.* A **456**, 1741–1758.

Moffatt, H. K. 1964*a* Viscous and resistive eddies near a sharp corner. *J. Fluid Mech.* **18**, 1–18.

Moffatt, H. K. 1964*b* Viscous eddies near a sharp corner. *Arch. Mech. Stosow.* **2**, 365–372.

Moffatt, H. K. 1980 The asymptotic behaviour of solutions of the Navier-Stokes equations near sharp corners. In *Approximation Methods for Navier-Stokes Problems*. Lecture Notes in Mathematics, vol. 771 (ed. R. Rautmann), pp. 371–380. Springer.

Moffatt, H. K. & Duffy, B. R. 1980 Local similarity solutions and their limitations. *J. Fluid Mech.* **96**, 299–313.

Moffatt, H. K. & Mak, V. 1999 Corner singularities in three-dimensional Stokes flow. In *IUTAM Symposium on Non-linear Singularities in Deformation and Flow*, pp. 21–26. Kluwer.

Sano, O. & Hasimoto, H. 1980 Three-dimensional Moffatt-type eddies due to a Stokeslet in a corner. *J. Phys. Soc. Japan* **48**, 1763–1768.

Shankar, P. N. 1997 Three-dimensional eddy structure in a cylindrical container. *J. Fluid Mech.* **342**, 97–118.

Shankar, P. N. 1998 Three-dimensional Stokes flow in a cylindrical container. *Phys. Fluids* **10**, 540–549.

Shankar, P. N. 2000 On Stokes flow in a semi-infinite wedge. *J. Fluid Mech.* **422**, 69–90.

Taylor, G. I. 1962 On scraping viscous fluid from a plane surface. In *Miszellangen der Angewandten Mechanik* (ed. M. Schäfer), pp. 313–315. Akademie.

Wakiya, S. 1976 Axisymmetric flow of a viscous fluid near the vertex of a body. *J. Fluid Mech.* **78**, 737–747.

Weidman, P. D. & Calmidi, V. 1999 Instantaneous Stokes flow in a conical apex aligned with gravity and bounded by a stress-free surface. *SIAM J. Appl. Maths* **59**, 1520–1531.